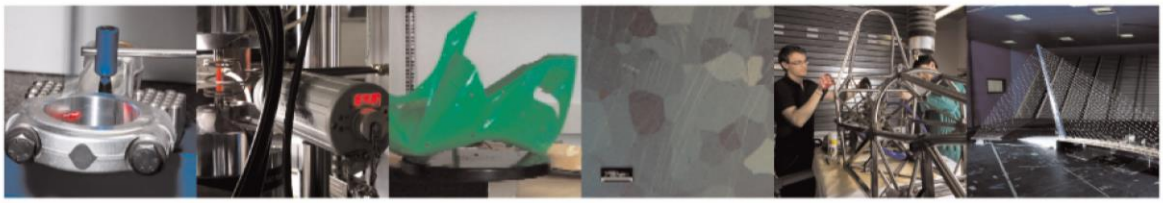

Process development and monitoring in stripping of a highly transparent polymeric paint with ns-pulsed fiber laser

Jasim, Halah A.; Demir, Ali Gökhan; Previtali, Barbara; Taha, Ziad A.

This is a post-peer-review, pre-copyedit version of an article published in OPTICS AND LASER TECHNOLOGY. The final authenticated version is available online at:
http://dx.doi.org/10.1016/j.optlastec.2017.01.031

Process development and monitoring in stripping of a highly transparent polymeric paint with ns-pulsed fiber laser

Halah A. Jasim[1], Ali Gökhan Demir[2*], Barbara Previtali[2], Ziad A. Taha[1]

[1] Institute of Laser for Postgraduate Studies, University of Baghdad, Iraq

[2] Department of Mechanical Engineering, Politecnico di Milano, Via La Masa 1, 20156 Milan, Italy

*Corresponding author: aligokhan.demir@polimi.it

Process development and monitoring in stripping of a highly transparent polymeric paint with ns-pulsed fiber laser

Abstract

Laser paint removal was studied with ns-pulsed fiber laser on the combination of 20 μm-thick, white polymeric paint and Al alloy substrate. The response of paint to single pulsed ablation was evaluated to measure the ablated zone dimensions. With this information, the effect of overlap, number of passes and pulse repetition rate was evaluated to investigate machining depth. Optical emission spectroscopy was used to investigate the machining behaviour as well as to propose monitoring strategies. The results showed that despite the high transparency of the paint, complete paint removal can be achieved with reduced substrate damage (Sa=1.3 μm). The emission spectroscopy can be used to identify removal completion as well as the reach of substrate material. The observations were also used to explain a paint removal mechanism based on thermal expansion of the paint and mechanical action provided by the plasma expansion from the substrate material.

Keywords: Polyester paint, aluminium alloy, optical emission spectroscopy, surface roughness

1. Introduction

Laser paint stripping provides several advantages being a non-contact process, not requiring solvents or abrasive particles [1-3]. Due to these advantages laser paint stripping and cleaning have become an appealing technique for electronics, aerospace, energy applications as well as art conservation. Several works have been published in the literature dealing with different paint/substrate combinations and employing different laser sources. The limitation of the damage on the substrate is determined by the interaction between the beam and paint. The substrate materials reported in literature vary greatly as both conductive and non-conductive substrates have been studied [3]. The used sources change as a function of absorptivity of the paint layers as excimer [4], diode [5], Nd:YAG [4,6-8],and CO_2 [7-12] lasers have been proposed. More recently long-pulsed and continuous fiber lasers have also been employed for the purpose [13]. Ultra-short pulsed lasers have been demonstrated to be highly effective by providing non-thermal machining conditions [14]. Water jet assisted laser paint stripping was also demonstrated by Madhukar et al employing a high power fiber laser running in the water jet stream to

enhance the process cleanliness [15]. As demonstrated in literature, paint stripping has been commonly applied with continuous wave (CW) sources and large beams in order to improve productivity. While paint removal is commonly applied to large components such as the ones in nuclear, automotive and marine applications, selective removal with a small spot suitable for micromachining can be useful for electronics and biomedical applications.

Several mechanisms have been proposed based on selective vaporization, spallation, transient surface heating and bond breaking [1]. Roberts demonstrated that the paint removal mechanism can vary from detachment to ejection depending on the absorptivity of the paint layer [4]. The direct absorption by the paint results in surface ablation that allows for high precision, yet low removal efficiency. Coating detachment can be achieved by transmitting the laser beam through the paint and interacting also with the substrate. This causes complete detachment of the paint. The author used high energy Nd:YAG laser sources with large beams for the process. Concerning paints with high transparency at the laser wavelength, detachment based removal can be further advantageous. Polymeric paints, depending on the colour additives, can be highly transparent to Nd.YAG and fiber laser wavelength (1 μm). With optimal processing strategy, ns-pulsed fiber lasers perform paint stripping in detachment mode, but maintain geometrical precision due to the limited and energy input in time as opposed to their CW counterparts and in space due to the small beam size reducing the size of interaction zone. In particular, the processed depth should be controlled carefully in order to avoid substrate damage.

The ns-pulsed fiber lasers have become a workhorse in laser micromachining applications for large scale industrial production. Some of the key processes involved are laser marking and engraving mainly applied on metallic materials. Their small footprint and reliable architecture are some of the most important aspects that provided an extensive use in industry. These properties are exploited for long and continuous operation as well as implementation with machining centres and/or industrial robots. Despite being an industrially accepted tool, to authors' knowledge there is no scientific work on their use and consecutive characterisation for paint stripping applications.

On the other hand, the research communities have mainly concentrated on the productivity aspect, control over the machining extent and depth has been treated sparingly. From this point of view, process monitoring plays an important role for process precision. Machining depth and the state of laser material

interaction can be linked to process indicators such as light [16,17] and acoustic [18] emission in the proximity of the process. These indicators are linked to plasma formation and shockwave expansion in laser ablation based processes [19]. Spectroscopy is a useful tool as it can provide wavelength resolved information depicting the changes in the physics of the process [20]. As a matter of fact, laser induced breakdown spectroscopy has been previously employed for pigment characterization [21], and can be used for process monitoring means as well.

In this work laser stripping of polyester based paint from Al alloy substrate is studied with a Q-switched fiber laser operating with ns pulse and emitting at 1064 nm wavelength. The paint/substrate pair constituted a challenging combination of high transparency at the paint layer and high reflectivity at the substrate. Process parameters were investigated to ensure complete paint removal without excessive substrate damage. In the initial phase, material removal was studied first a single pulsed emission. Later the effect of overlap, pulse repetition rate and number of passes on machining depth and surface roughness was studied. Optical emission spectroscopy was employed for process monitoring in order to avoid substrate damage. In particular, emission characteristics were linked to machining depth.

2. Materials and methods

The substrate material used in the present investigation was EN AW 5005A aluminium alloy, with the chemical composition as shown in Table 1. A polymeric paint consisting of polyester with presence of polyamide was applied on the substrate material (Novelis, Bresso, Italy). Before the painting procedure, the surface degreased in alkaline bath and pre-coated with Ti and Zr (~2 μm). The paint was applied in two layers consisting of 5 μm and 15 μm thickness, giving a total of 20 μm. The paint appeared with a white colour and its transmissivity at near infrared region was >90%.

Table 1. Nominal chemical composition of EN AW 5005A aluminium declared by the producer.

Element	Si	Fe	Cu	Mn	Mg	Cr	Zn	Others	Al
wt%	0.3	0.45	0.05	0.15	0.7-1.1	0.1	0.2	0.15	Bal.

The experiments were carried out with a pulsed ytterbium fiber laser (YLP- 1/100/50/50 from IPG Photonics, Cambridge, MA, USA) operating at 1064 nm wavelength. The collimated beam diameter 5.9 mm with beam quality M^2=1.7. The laser beam was manipulated with a scanner that housed a 100 mm f-theta lens (TSH 8310D, from Century Sunny, Beijing, China) capable to move at speeds up to 6000 mm/s. The laser beam was focused with focal length 100 mm when the laser diameter 39 μm. The system generates 250 ns pulses at a repetition rates up to 80 kHz, and the maximum pulse energy reaches to 1.12 mJ. A spectrometer was integrated to the machining system to monitor the process emission (AvaSpec 3648-USB2, from Avantes, Apeldoorn, Netherlands). Laser emission was suppressed using and optical filter (FESH1000 from Thorlabs, Newton, NJ).

Machining depth and surface roughness of the samples were measured by focus variation microscopy (Infinite Focus from Alicona, Graz, Austria). For surface machining depth and average roughness of the surface (Sa) 10X objective was employed, with estimated vertical and laterals resolutions being 1.05 μm and 7.73 μm respectively. Machining depth was measured as the average height of the surface profile Surface morphology was also analysed using scanning electron microscope (EVO-50 from Carl Zeiss, Oberkochen,Germany).

3. Experimental procedure

Surface machining with pulsed lasers is applied as explained schematically in Figure 1. The laser pulses are overlapped on the scan direction and between adjacent scan lines. The laser energy (E) determines the ablated zone extent, hence the diameter of each the pseudo tool (D). The overlapping on the scan direction (O_x%) can be calculated from the following expression.

$$O_x\% = 1 - \frac{v}{D(E)\cdot PRR} \qquad \text{Eq.(1)}$$

where D(E) is the diameter of the ablated zone by a single pulse, which depends on laser pulse energy (E); v is the scan speed; and PRR is the pulse repetition rate. Similarly, on the Y direction the laser pulses will overlap as a function of pitch (p). Accordingly, the overlap between the adjacent lines can be calculated from:

$$O_y\% = 1 - \frac{p}{D(E)} \qquad \text{Eq.(2)}$$

For paint stripping purposes, the overlap can be as small as possible, in order to reduce the machining time. In this study, the overlapping in both directions was taken equal in order to evaluate the effect of this parameter ($O_x\%= O_y\%= O\%$).

The experiments were carried out in two phases. Initially, material's response to the laser emission was characterized under single pulsed ablation. Laser pulse energy was varied between 0.16 and 1.12 mJ and the focal plane was positioned on the material surface. Ablated zone diameter as function of pulse energy (D(E)) was determined. Machining depth (h) was also measured to investigate the effect of pulse energy on the paint removal in depth. The energy level for further studies was determined at this phase. In the second phase, with fixed pulse energy (E) and corresponding ablation diameter (D(E)), the effect of pulse repetition rate (PRR), overlap (O%), and number of passes (N) was assessed. Pulse repetition rate was fixed at 2 levels, 20 kHz and 50 kHz. Overlap was varied between 25% and 75%. For each level of overlap, corresponding scan speed (v) and pitch (p) were calculated using Eq.(1) and Eq.(2) respectively. Single pass and two passes (N) were tested. Machining depth (h) as well as average surface roughness (Sa) was measured to assess the efficacy of the process. Spectroscopy was applied in order to assess the changes in the optical emission spectra while machining on and beyond the paint. Integral of the overall emission spectra (I_{tot}) and emission intensity of chosen lines were analysed. Machining depth was assessed by realizing patches of 3 x 3 mm^2 on the material surfaces, whereas monitoring was applied while machining single track of 10 mm length. A single spectrum was registered at each laser pass with 100 ms integration time. The details of the experimental plan in this phase are explained in Table 2.

Table 2. Fixed and varied parameters in the second phase of the experiments.

Fixed parameters		
Focal position	h_f (mm)	0
Pulse energy	E (mJ)	0.16
Varied parameters		
Overlap	O%	From 25 to 75 with increment of 5
Pulse repetition rate	PRR (kHz)	20, 50
Number of passes	N	1, 2
Measured variable		
Machining depth	h (µm)	
Average surface roughness	Sa (nm)	
Integral of emission spectra	I_{tot} (AU)	

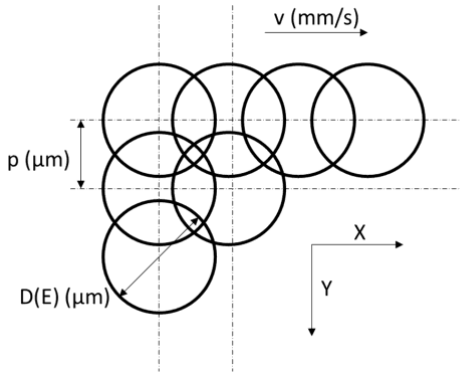

Figure 1. Schematic representation of machining with pulsed lasers showing overlapping in X and Y directions.

4. Results

4.1. Determination of material response to single pulse ablation

Figure 2 depicts the morphology of ablation zone under a single laser pulse with variable pulse energy. It can be observed that the ablated zone morphology deviates from the circular shape of the laser beam. With increased energy content the ablated zone increases as expected from the process. however, the ablated zone depth shows stable behaviour until around 0.73 mJ. The measured values of ablation diameter (D) and the depth (h) with respect to the variation in laser energy is presented in Figure 3. The measured ablated area diameters follow the usual trend explained by the ablation threshold model. Fitting the data using the analytical expression it is possible to estimate both the laser beam radius (w_0) and ablation threshold fluence (F_{th}).

$$D^2 = 2w_0^2 \ln\left(\frac{\frac{2E}{w_0^2\pi}}{F_{th}}\right) \qquad \text{Eq(3)}$$

As seen with the dashed lines in Figure 4 the model fits the data very well. On the other hand, the estimated beam radius was 78±10 µm and ablation threshold was 4.2±0.9 J/cm^2. The estimated radius is by far larger than the used focus laser beam (w_0=19.5 µm). This fact is attributed to the difference in laser material interaction. Due to low absorbance of the laser wavelength, the material is expected to transmit a large portion of the beam inside the coating. Accordingly, the interaction is no longer limited to the surface, but is extended to the depth as well. Hence, the material senses a heat field larger than the actual laser beam at focal position. As a matter of fact, the material removal mechanism was observed to be based on particle ejection. Thus, the ablated region depth is constantly around the coating

thickness at 10 µm below 0.80 mJ. Above 0.80 mJ an abrupt shift in the machining depth to above the paint thickness is seen.

For the second phase of the experiments, pulse energy was fixed at 0.16 mJ, which provided an average ablation diameter of 39.4±9.0 µm and machining depth of 9.8±1.3 µm. The low pulse energy provided control over the machining depth, since preliminary experiments with higher energy levels showed uncontrollable process due to excessive machining depth.

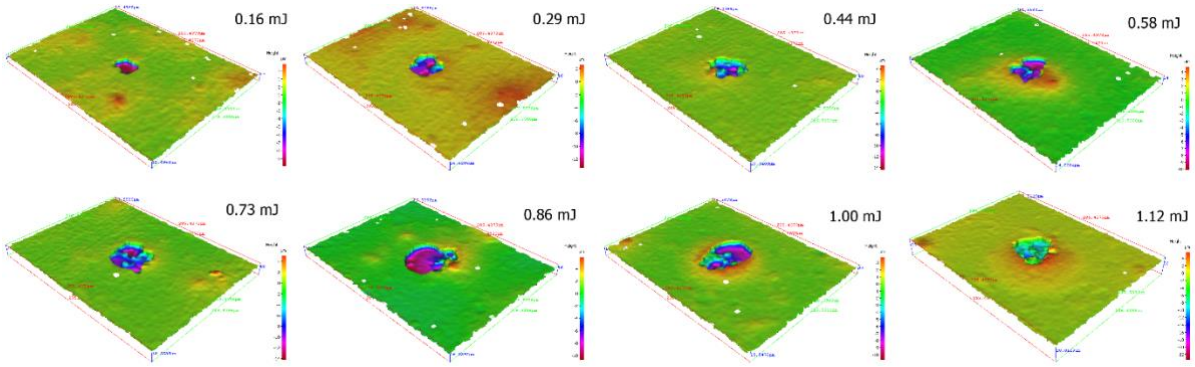

Figure 2. Focus variation microscopy images showing the evolution of ablation zone dimensions as a function of pulse energy in single pulse ablation.

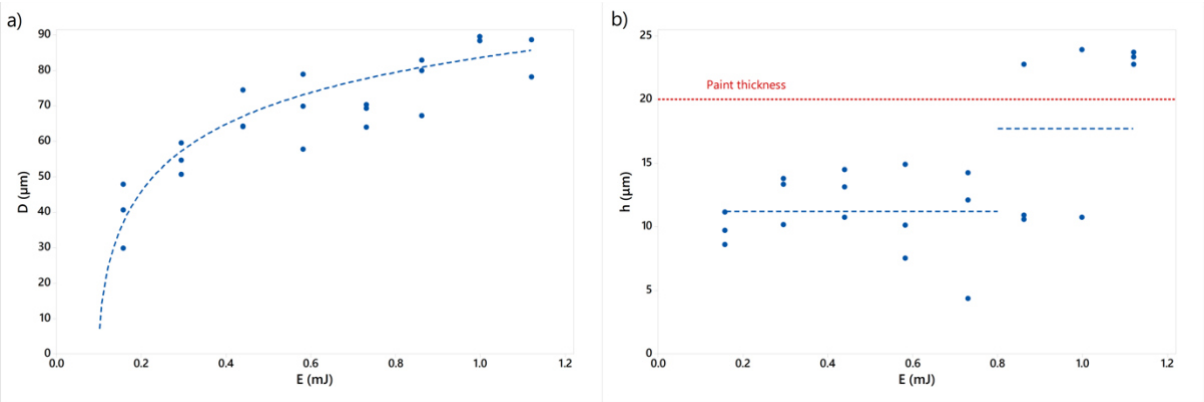

Figure 3. a) Ablation diameter (D) laser pulse energy, the dashed line depicts the fitted ablation threshold model. b) Machining depth (h) as a function of laser pulse energy, the dashed lines represent group means between 0.16-0.73 mJ and between 0.86-1.12 mJ.

4.2. Effect of process parameters on machining depth and surface quality

Figure 4 exhibits SEM images of the surfaces after a single pass of laser irradiation applied with different overlap and pulse repetition rate levels. It can be seen that with 25% overlap, the paint is still

present on the surface with partial removal. At 50% overlap there is no paint residue on the surface and the Al substrate is partially machined. At 75% overlap, Al substrate is machined and the surface presents recast layer of the substrate material, commonly present in laser micromachining with ns pulses.

The experiments showed that the machining depth varied below and in the proximity of the paint thickness. Below the paint thickness, incomplete removal resulted in a reduced average height. As the overlap increases a more homogenous surface profile is present as also seen in Figure 4.

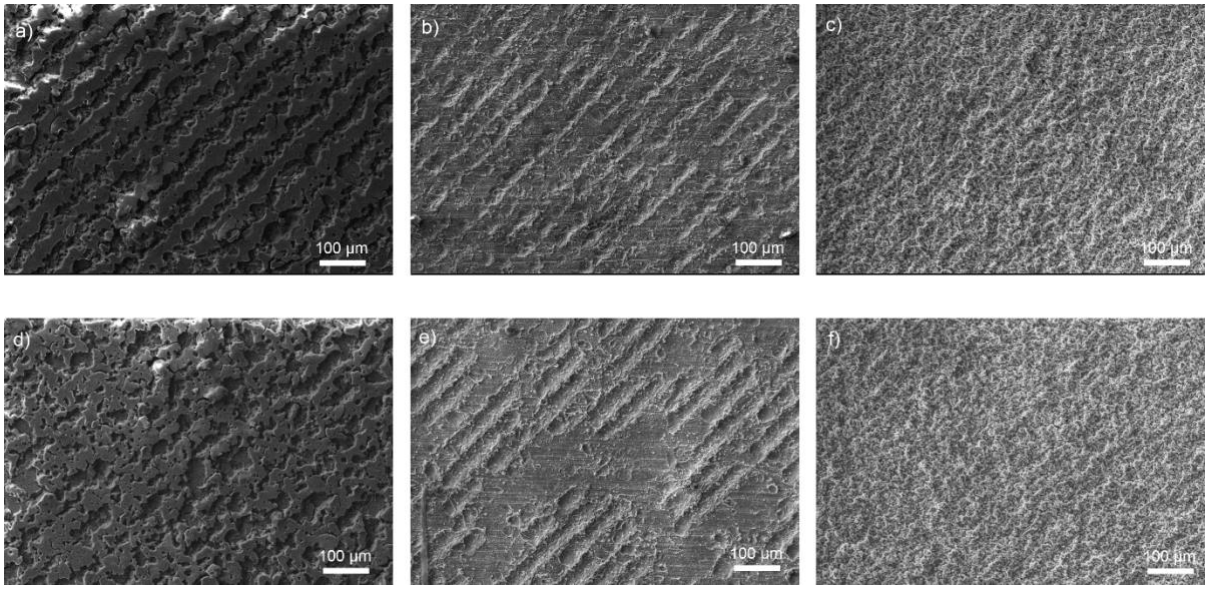

Figure 4. SEM of surfaces after a single pass applied with a) O=25%, PRR=20 kHz, b) O=50%, PRR=20 kHz, c) O=75%, PRR=20 kHz, d) O=25%, PRR=50 kHz, e) O=50%, PRR=50 kHz, f) O=75%, PRR=50 KHz.

The change of machining depth as function of process parameters is shown in Figure 5. In particular, the machining depth follows a similar trend for all PRR and N levels. At single pass (N=1), the complete removal is achieved around 50% overlap for both PRR levels. With 2 passes (N=2), the required overlap level for complete paint removal reduces to around 45%. It can be noted that, below the paint thickness (20 µm) the machining depth increases following an exponential behaviour. On the other hand, the increase of pulse repetition rate shows a relative increase of machining depth above the paint thickness. In particular, PRR at 50 kHz with 2 passes shows a more rapid increase above 40% overlap. This is expected to be due to the previously mentioned thermal incubation effect. The smaller effect of number of passes (N) also suggests that surface heating is a predominant factor. As a matter of fact, distinct

passes arrive with a time delay on the same machined spot. For this reason, a single pass applied at 50% overlap results in higher machining depth compared to 2 passes applied at 25%.

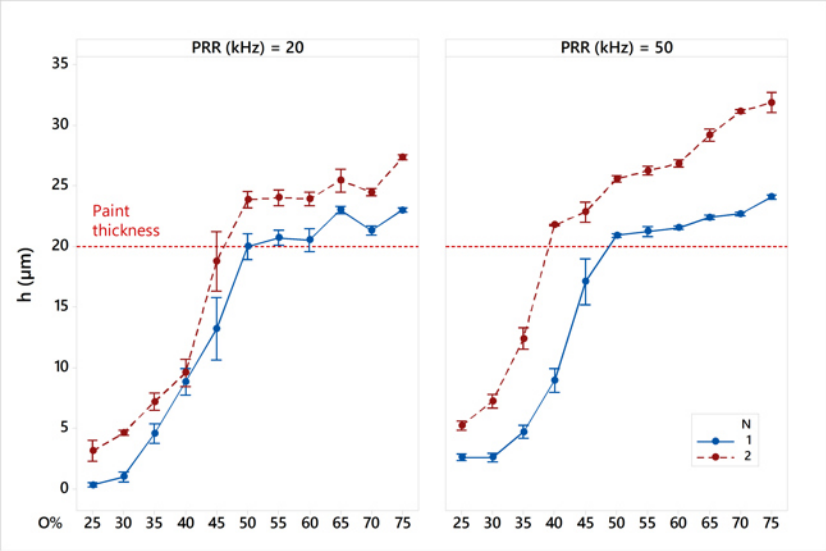

Figure 5. Machining depth as function of process parameters. Error bars represent standard error for each group, dashed lines depict trend only.

The change in machining rate below and above paint thickness can be attributed to the change in ablation mechanisms, when Al substrate is reached. Despite sufficient laser energy, ablation of Al with the present overlap levels is difficult. Laser engraving of metallic substrates is commonly done at high overlap levels (>90%) in order to achieve homogenous surfaces. In fact, the calculated overlap values refer to ablation diameters obtained on the paint, which will be considerably different on the Al substrate due to the change of material physical properties. according to the measurements, the paint removal can be applied at an overlap around 50% with a single pass. In order to improve productivity pulse repetition can be used at 50 kHz, which results in paint stripping coverage of 11.7 cm^2/min, compared to 4.7 cm^2/min achieved with 20 kHz. A key process indicator in paint stripping is removal efficiency defined as:

$$RE = \frac{V_p}{t_{tot} \cdot P} \qquad \text{Eq.(4)}$$

where V_p is the removed paint volume, t_{tot} is the process time and P is the laser power [22]. The parameter indicates the process productivity per laser watt employed, therefore considers also the thermal load on the substrate material. In the optimal conditions, the RE values is at 2.9 cm^3/min/kW in

this work. Ream [22] also provided industrial benchmark values of *RE* for white paints commonly applied in the aviation industry. CW fiber lasers are found to be problematic due to the high thermal load, and the corresponding industrial benchmark is 2.3 cm^3/min/kW. The same work reports the *RE* value for a similar Q-switched fiber. Accordingly, in the present work a moderate improvement in removal efficiency is achieved without generating high thermal stress on the material. It should be duly noted that the *RE* provided by CO_2 laser is 9 cm^3/min/kW, due to the improved absorption.

Figure 6 shows the average surface roughness measurements as a function of process parameters. Evidently, the average surface roughness Sa increases to above 10 µm, as the overlap increases and then drops to values below 5 µm after reaching the peak (Figure 8.a). This is due to the partial removal of the paint at lower overlap levels, which increases the surface roughness. As shown in Figure 8.b the surface roughness is directly linked to the machining depth. As the average machining depth increases surface roughness increases as well. At this point, surface is composed of partially removed paint and Al substrate. Once the paint removal is complete, surface roughness is composed of the machined Al substrate topography only. The results also imply that the use of higher pulse repetition rate and low number of passes is favourable for maintaining a lower surface roughness. Using 50 kHz pulse repetition rate with 50% overlap and a single pass results in Sa=1.33 µm

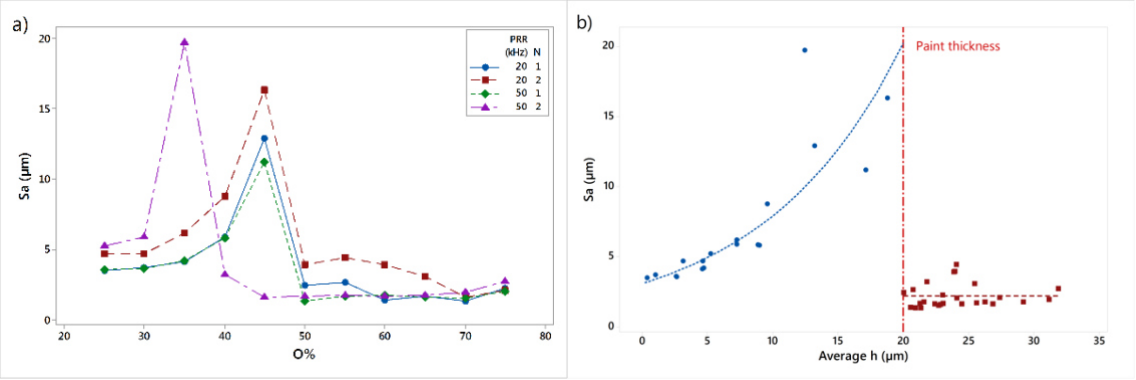

Figure 6. a) Average surface roughness (Sa) as a function of process parameters. b) Relationship between machining depth (h) and average surface roughness (Sa).

4.3. Monitoring of machining depth with OES

Figure 7 shows the emission spectra obtained with different overlap levels during the first and second passes. Overall, the spectra are composed of several peaks in the visible region and background

contribution with a hump form. The peaks are less visible at low overlap levels. It is expected that at low overlap levels laser is partially transmitted to the metallic substrate, which should cause very weak ionization and the stronger component of the spectra is the background caused by thermal radiation. Increased overlap and number of passes generates stronger peaks, whereas the background increases as well. This shows that ionization of the substrate material becomes predominant, however thermal process also increases. In Figure 7, some of the emission peaks were identified as ions belonging to elements found on the substrate material (Al and Fe) and surface treatment (Ti). Because Al I and II emission lines are predominantly present in the UV region, which has could not be measured with the present setup, only three lines belonging to Al II could be identified [22]. Three Fe I lines belonging were identified around 497 and 504 nm. Together with the Al II line at 500.1 nm, the Fe I lines showed higher increase with overlap and number of passes. On the other hand, Ti I lines around 589.9 and 625.8 nm were found to be dominant peaks with lower overlaps. The combined evaluation of 497-504 nm and 589-626 nm bands can further enrich the spectroscopic analysis. While the 589-626 nm shows a superficial interaction of the laser beam with the substrate, the 497-504 nm shows deeper interaction with the substrate. Hence, the 497-504 nm band rapidly increases once, paint removal is complete and substrate is being machined.

Figure 8 represents the total spectrum intensity as the sum off all intensity lines as a function of average processing depth. The figure has been divided in two regions showing total intensity while machining below and above the paint thickness. Below the paint thickness, the increase of total intensity follows a slow slope. After the complete removal of the paint the total intensity increases much more rapidly. A threshold total intensity around $1.5 \cdot 10_6$ could be identified, above which the paint removal is completed. This approach can be used monitoring the processing depth, hence prevent excessive substrate damage from occurring. For a faster monitoring response, a photodiode integrating the emission spectrum can be employed.

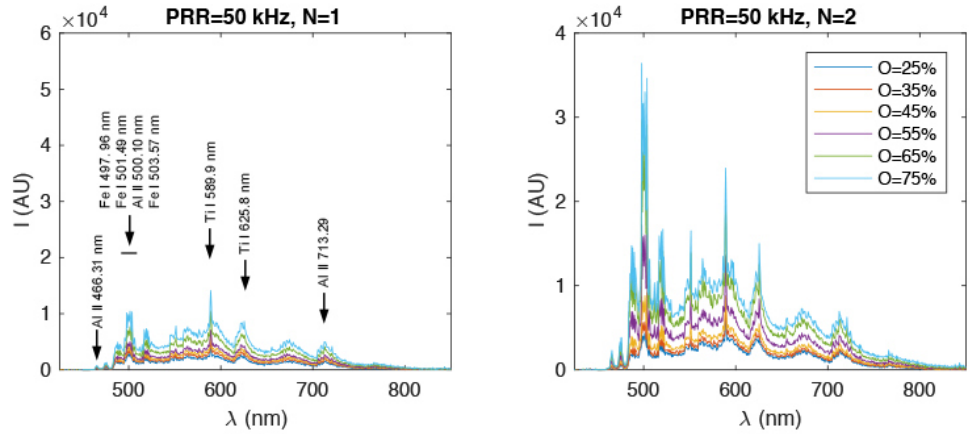

Figure 7. Emission spectra during laser paint stripping with different overlap levels after first and second passes.

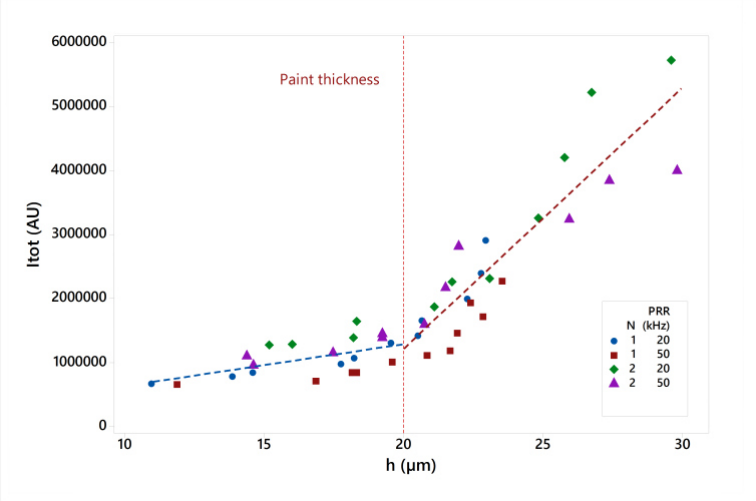

Figure 8. Total emission intensity as a function of machining depth.

5. Conclusions

The objective of the present investigation was to study the paint removal process in a combination of 20 μm thick polyester white paint applied on 5005A Al alloy with a pulsed fiber laser emiting at 1064 nm. In the experimental study, the overlapping factor on both axis was varied together by using the average ablated zone diameter per energy level. In the optimal conditions, the process yields a paint removal rate of 11.7 cm^2/min and removal efficiency of 2.9 cm^3/min/kW. Surface roughness was

measured to be Sa=1.3 μm after the completion of the paint removal (h>20 μm), which gradually increased as a function of machining depth due to the roughening of Al substrate.

Optical emission spectroscopy was applied to observe the process emission during single track paint stripping. The analysis revealed ionization peaks belonging to elements found on the surface pre-coating and substrate, as well as a thermal background. Two distinct regions were identified at 497-504 nm and 589-626 nm bands. The strength of the first band increased more rapidly with the increase of processing depth indicating ionization of substrate elements Al and Fe. The second one was found to be present in all cases, however, its strength increased less rapidly indicating surface pre-coating Ti. The total intensity of the spectra was found to suitably correlate with the machining depth.

Overall the results show that use of ns-pulsed fiber laser is capable of removing a highly transparent polymeric paint from the Al substrate without excessive substrate damage. The benchmark results depict that ns-pulsed fiber laser is less productive compared to the CO_2 laser in removing the highly transparent paint. In terms of precision, the use of a smaller beam provides higher resolution over the scan plane. The proposed monitoring technique can be beneficial for improving the damage on the substrate material. The robust architecture, fiber delivery and small footprint aspects can be further exploited to overcome the productivity issue by implementing multiple scan heads installed to robotic arms, expanding the application to larger surface areas.

Acknowledgements

The authors wish to express their gratitude to the Iraqi Ministry of Higher Education and scientific research for partially funding this research. The authors also gratefully acknowledge Novelis Italia Spa for providing the painted Al samples.

References

1. W. Steen, Laser Material Processing, 4th Ed, Springer-Verlag, London, 2010
2. K. Liu, E. Garmire, "Paint Removal Using Lasers", Appl Optics 34 (1995) 4409 – 4415,
3. Sp.G. Pantelakis , Th.B. Kermanidis , G.N. Haidemenopoulos, "Mechanical behavior of 2024 A1 alloy specimen subjected to paint stripping by laser radiation and plasma etching", Theor Appl Fract Mec, vol. 25, pp. 139-146, 1996
4. D.E. Roberts, Pulsed Laser Coating Removal by Detachment and Ejection, Appl Phys A, 79 (2004) 1067–1070
5. M. Barletta , A. Gisario, V. Tagliaferri, Advance in Paint Stripping from Aluminium Substrates, J. Mater. Process. Technol. 173 (2006) 232–239.
6. F. Brygo , Ch. Dutouquet , F. Le Guern , R. Oltra , A. Semerok , J.M. Weulersse, Laser Fluence, Repetition Rate and Pulse Duration Effects on Paint Ablation, Appl Surf Sci, 252 (2006) 2131–2138
7. M. L. Klingenberg, D.A. Naguy, T.A. Naguy, R.J. Straw, C. Joseph, G.A. Mongelli, G.C. Nelson, S.L. Denny, and J.J. Arthur. Transitioning Laser Technology to Support Air Force Depot Transformation Needs, Surf Coat Techc 202 (2007) 45–57
8. Sp.G. Pantelakis , G.N. Haidemenopoulos, Effect of Novel Paint Removal Processes on the Fatigue Behavior of Aluminum Alloy 2024, Surf Coat Tech, 106 (1998) 198–204
9. A. Tsunemi, A. Endo, D. Ichishima "Paint Removal from Aluminum and Composite Substrate of Aircraft by Laser Ablation Using TEA CO_2 Lasers", Proceedings of High-Power Laser Ablation (1998) 1018-1022
10. F J Prinsloo, S P van Heerden, E. Ronander, Efficient TEA CO_2 laser based coating removal system, Proceedings of XVI International Symposium on Gas Flow, Chemical Lasers, and High-Power Lasers (2007) 63462Q-63462Q
11. J. F. Coutouly, P. Deprez, F. Breaban, J. Paul Longuemard, Optimisation of a Paint Coating Ablation Process by CO_2 TEA laser: Thermal Field Modeling and Real-Time Monitoring of the Process, J Mater Proc Tech 209 (2009) 5730–5735

12. M. Kumar, P. Bhargava, A. K. Biswas, Shasikiran Sahu, V. Mandloi, M. O. Ittoop, B. Q. Khattak, M. K. Tiwari, and L. M. Kukreja, Epoxy-paint stripping using TEA CO_2 laser: Determination of threshold fluence and the process parameters, Opt Laser Tech, 46 (2013) 29–36
13. Y. K. Madhukar, S. Mullick, D. K. Shukla, S. Kumar, A. K. Nath, Effect of Laser Operating Mode in Paint Removal with a Fiber Laser, Appl Surf Sci 264 (2013) 892– 901
14. A.V. Rode, D. Freeman, K.G.H. Baldwin, A. Wain, O. Uteza, Ph. Delaporte, Scanning The Laser Beam for Ultrafast Pulse Laser Cleaning of Paint, Appl Phys A 93 (2008) 135–139
15. Y. K. Madhukar, S. Mullick, A. K. Nath, Development of a Water-Jet Assisted Laser Paint Removal Process, Appl Surf Sci 286 (2013) 192– 205
16. V. Kanicky, J. Musil, and J.-M. Mermet, Determination of Zr and Ti in 3- mu m-Thick ZrTiN Ceramic Coating Using Laser Ablation Inductively Coupled Plasma Atomic Emission Spectrometry, *Appl. Spectrosc.*, 51(7) (1997) 1037–1041
17. F. Leguern, F. Brygo, P. Fichet, E. Gauthier, C. Hubert, C. Lascoutuna, D. Menut, S. Mousset, A. Semerok, and M. Tabarant, Co-deposited layer characterisation and removal control by optical emission spectroscopy coupled to nano-second laser ablation, Fusion Eng. Des., 81 (8–14) (2006) 1503–1509
18. T. Kurita, A study of processed area monitoring using the strength of YAG laser processing sound, *J. Mater. Process. Technol.* 112(1) (2001) 37–42
19. S. H. Jeong, R. Greif, and R. E. Russo, Shock wave and material vapour plume propagation during excimer laser ablation of aluminium samples, *J. Phys. D. Appl. Phys.*, 32 (19) (1999) 2578–2585
20. C. Aragón and J. A. Aguilera, Characterization of laser induced plasmas by optical emission spectroscopy: A review of experiments and methods, *Spectrochim. Acta - Part B At. Spectrosc* 63 (9) (2008) 893–916
21. D. A. K. Melessanaki, V. Papadakis, C. Balas, "Laser induced breakdown spectroscopy and hyper-spectral imaging analysis of pigments on an illuminated manuscript," *Spectrochim. Acta Part B* 56 (2001) 2337–2346

22. S. Ream, Laser system strips paint from full-size aircraft. Industrial Laser Solutions, 31(5) (2016), 5-10

23. A.Kramida, Y. Ralchenko,.J. Reader, and NIST ASD Team (2015). NIST Atomic Spectra Database (ver. 5.3), [Online]. Available: http://physics.nist.gov/asd [2016, April 8]. National Institute of Standards and Technology, Gaithersburg, MD.

List of figures

Figure 1. Schematic representation of machining with pulsed lasers showing overlapping in X and Y directions.

Figure 2. Focus variation microscopy images showing the evolution of ablation zone dimensions as a function of pulse energy in single pulse ablation.

Figure 3. a) Ablation diameter (D) laser pulse energy, the dashed line depicts the fitted ablation threshold model. b) Machining depth (h) as a function of laser pulse energy, the dashed lines represent group means between 0.16-0.73 mJ and between 0.86-1.12 mJ.

Figure 4. SEM of surfaces after a single pass applied with a) O=25%, PRR=20 kHz, b) O=50%, PRR=20 kHz, c) O=75%, PRR=20 kHz, d) O=25%, PRR=50 kHz, e) O=50%, PRR=50 kHz, f) O=75%, PRR=50 KHz.

Figure 5. Machining depth as function of process parameters. Error bars represent standard error for each group, dashed lines depict trend only.

Figure 6. a) Average surface roughness (Sa) as a function of process parameters. b) Relationship between machining depth (h) and average surface roughness (Sa).

Figure 7. Emission spectra during laser paint stripping with different pulse repetition rate and overlap levels after first and second passes.

Figure 8. Total emission intensity as a function of machining depth.

List of tables

Table 1. Nominal chemical composition of EN AW 5005A aluminium declared by the producer.

Table 2. Fixed and varied parameters in the second phase of the experiments.